

## Mechanism of Interaction of Monovalent Ions with Phosphatidylcholine Lipid Membranes

Robert Vácha,<sup>\*,†,‡</sup> Piotr Jurkiewicz,<sup>\*,§</sup> Michal Petrov,<sup>†</sup> Max L. Berkowitz,<sup>||</sup>  
Rainer A. Böckmann,<sup>⊥</sup> Justyna Barucha-Kraszewska,<sup>§</sup> Martin Hof,<sup>§</sup> and Pavel Jungwirth<sup>†</sup>

*Institute of Organic Chemistry and Biochemistry, Academy of Sciences of the Czech Republic and Center for Biomolecules and Complex Molecular Systems, Flemingovo nám. 2, 16610 Prague 6, Czech Republic; Department of Chemistry, University of Cambridge, Lensfield Road, Cambridge, CB21EW, United Kingdom; J. Heyrovský Institute of Physical Chemistry, Academy of Sciences of the Czech Republic, v. v. i., Dolejškova 3, 18223 Prague 8, Czech Republic; Department of Chemistry, University of North Carolina, Chapel Hill, North Carolina 27599; and Computational Biology, Department of Biology, University of Erlangen-Nürnberg, 91058 Erlangen, Germany*

Received: March 16, 2010; Revised Manuscript Received: June 3, 2010

Interactions of different anions with phospholipid membranes in aqueous salt solutions were investigated by molecular dynamics simulations and fluorescence solvent relaxation measurements. Both approaches indicate that the anion–membrane interaction increases with the size and softness of the anion. Calculations show that iodide exhibits a genuine affinity for the membrane, which is due to its pairing with the choline group and its propensity for the nonpolar region of the acyl chains, the latter being enhanced in polarizable calculations showing that the iodide number density profile is expanded toward the glycerol level. Solvent relaxation measurements using Laurdan confirm the influence of large soft ions on the membrane organization at the glycerol level. In contrast, chloride exhibits a peak at the membrane surface only in the presence of a surface-attracted cation, such as sodium but not potassium, suggesting that this behavior is merely a counterion effect.

## Introduction

It has been observed in numerous experimental and theoretical studies that addition of salts changes the properties of lipid membranes.<sup>1–11</sup> Molecular dynamics simulations demonstrated salt-induced changes in lateral diffusion of phospholipids, head-group tilt, membrane thickness, etc., which were specific for different cations.<sup>1–3,5,11</sup> Fewer computational studies investigated the effect of anions and either reported anionic influence on membranes<sup>4</sup> or similar changes for all sodium halide salt solutions (although it was observed that larger anions penetrate slightly more into the membrane than sodium).<sup>11</sup> In contrast, experiments primarily focused on the effects of anions that have been shown to follow the Hofmeister series.<sup>12</sup> For example, experiments on vesicles swelling in KCl and KBr solutions have been rationalized in terms of the enhanced presence of anions at the membrane surface.<sup>7</sup> Recent experiments on DPPC monolayers with sodium salt solutions showed that, while an anion adsorption explains well results for sodium salts with larger halides, those for NaF could not be fitted by such a model. A model which fits the data for all sodium salts invokes both anion adsorption and a simultaneous sodium complexation with lipids.<sup>9,10</sup> Such an interaction of sodium with lipid membranes was previously confirmed by fluorescence spectroscopy, which showed a slowdown in lateral diffusion of lipids and different mobility at the headgroup region.<sup>11,13</sup>

An important step toward understanding the interactions of biomolecules with ions in salt solution has been made by introducing the so-called “law of matching water affinities”.<sup>14,15</sup> This law is an empirical rule that relates the propensity of oppositely charged moieties to form contact pairs in water solution and their hydration properties. Typically, ionic species which tend to pair the most in water are those with matching hydration free energies (i.e., roughly speaking, sizes). This tendency of like-sized oppositely charged species to pair in water has been also observed in simulations<sup>16–20</sup> and was rationalized within a dielectric continuum model recently.<sup>21</sup>

In this paper, we compare different salts by varying both cations and anions: this allows us to distinguish between different mechanisms responsible for ion–membrane interaction. Moreover, we present, for the first time, results from the simulation of membrane in a salt solution performed using a polarizable force field. It has been recently shown that the inclusion of polarizability is important for the description of anions at water/hydrophobic interface, where local concentrations of large and polarizable ions can be enhanced compared to the aqueous bulk.<sup>22–26</sup> We paralleled our calculations with fluorescence solvent relaxation measurements using Laurdan,<sup>27</sup> thus providing direct information about the influence of such ions on the polarity and mobility of lipid bilayer at the glycerol level.<sup>28</sup>

## Methods

**Computation.** Molecular dynamics (MD) simulations were performed using the GROMACS program package version 3.3.1.<sup>29</sup> Four systems were simulated: each consisted of 72 DOPC lipid molecules, 2627 water molecules, 50 cations, and 50 anions, representing a ~1 M solution of 1:1 salt. The salt in our simulations was KI, NaI, KCl, or NaCl. The simulations were carried out for 200 ns with a 2 fs time step. The first 80

\* To whom correspondence should be addressed. E-mail: rv260@cam.ac.uk (R.V.); piotr.jurkiewicz@jh-inst.cas.cz (P.J.).

<sup>†</sup> Institute of Organic Chemistry and Biochemistry, Academy of Sciences of the Czech Republic and Center for Biomolecules and Complex Molecular Systems.

<sup>‡</sup> University of Cambridge.

<sup>§</sup> J. Heyrovský Institute of Physical Chemistry, Academy of Sciences of the Czech Republic.

<sup>||</sup> University of North Carolina.

<sup>⊥</sup> University of Erlangen-Nürnberg.

ns were used for equilibrating the system and the following 120 ns for sampling. We employed the canonical NP $\gamma$ T ensemble with the surface tension of 22 mN/m in the membrane plane ( $xy$ -plane) and pressure of 1 atm in the perpendicular direction ( $z$ -axis). This particular value of the surface tension was chosen such as to match the experimental area per lipid.<sup>30</sup> The temperature was kept at 310 K using the Berendsen thermostat. Additional details concerning the force field and properties evaluation can be found in our previous paper,<sup>11</sup> where density profiles of ions of NaCl, KCl, and NaI salts solutions next to a DOPC membrane were studied.

In order to investigate the possible effect of the polarizability, we also performed a 20 ns long simulation of a DOPC membrane in a 1 M KI solution using a polarizable force field. The system setup was the same as in the nonpolarizable case, except that we employed the canonical NVT ensemble with the same value of volume as in simulations with the nonpolarizable force field. We could not perform polarizable simulations in a constant surface tension ensemble, because we do not know what value of surface tension one needs to use in order to get an experimental area per headgroup in simulations with polarizable force field. To get such information requires immense computational resources due to the use of a polarizable force field. The initial configuration in the polarizable simulation was taken from the end of a 200 ns nonpolarizable simulation. For water we employed the polarizable POL3 model<sup>31</sup> and polarizable ion parameters were taken from references.<sup>23,32</sup> The polarizable all-atom force field for the DOPC lipid was developed in a similar way as the nonpolarizable one, being based on generalized AMBER force field.<sup>30</sup> The partial charges of the DOPC molecule were calculated using density functional theory with the B3LYP functional and the cc-pvtz basis set.

**Experiment.** 1,2-Dioleoyl-*sn*-glycero-3-phosphocholine (DOPC) was purchased from Avanti Polar Lipids, Inc. (Alabaster, AL). 6-Dodecanoyl-2-dimethylaminonaphthalene (Laurdan) was obtained from Invitrogen (Eugene, OR). Salts (NaCl, NaBr, NaI, NaSCN, NaClO<sub>4</sub>), supplied by Sigma-Aldrich (St. Louis, MO), were dissolved in Milli-Q water (Millipore, Etten-Leur, The Netherlands).

Large unilamellar vesicles were prepared by the extrusion method. DOPC and Laurdan were mixed in chloroform in a 1:100 dye to lipid molar ratio. Chloroform was evaporated under a stream of nitrogen and then under vacuum for at least 2 h. The resulting dry lipid film was suspended in the chosen salt solution, vortexed for 4 min, and extruded through polycarbonate membranes (Avestin, Ottawa, Canada) with a pore diameter of 100 nm. The resulting suspension was measured in 1 cm quartz cuvette thermostated by circulating water at 10 °C. For each sample, a steady-state fluorescence spectrum and a series of fluorescence decays for emission wavelengths from 400 to 540 nm (with a 10 nm step) were recorded on a Fluorolog 3 (Jobin Yvon) and on an IBH 5000 U SPC equipped with an IBH laser diode NanoLED 11 and a cooled Hamamatsu R3809U-50 microchannel plate photomultiplier, respectively. From the measured data the time-resolved emission spectra (TRES) were reconstructed and analyzed. The total emission shift  $\Delta\nu$  and the mean integrated relaxation time  $\tau_i$ , which reflect polarity and mobility of probe environment at the glycerol level of phospholipid bilayer, respectively, were calculated as previously described.<sup>11</sup>

## Results

**Computation.** Results for DOPC in four different salt solutions, NaCl, KCl, NaI, or KI, are compared to each other

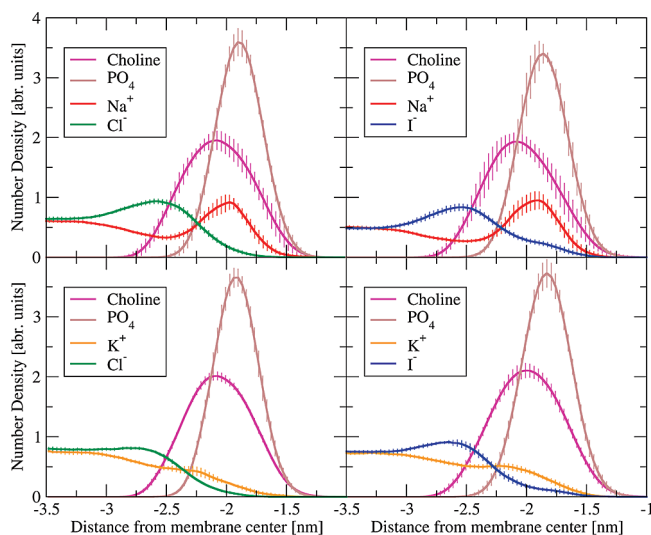


**Figure 1.** Ion density profiles in four different 1 M salt solutions (NaCl, NaI, KCl, and KI) next to a DOPC membrane. For easier identification of the headgroup region, partial density profiles of choline and phosphate groups are also depicted. Data were averaged over the two equivalent halves of the membrane over 120 ns.

in Figure 1. Here, the ion number density profiles along the axis perpendicular to the membrane are plotted. The focus is on the headgroup region, where ion profiles are strongly nonmonotonous, reflecting the complexity of the membrane/solution interface. For easier identification of the individual regions of the system, the partial density profiles of choline and phosphate groups of DOPC are also depicted. Below we provide a description of the ionic profiles for individual salts.

**NaCl.** The densities of both ions are enhanced at the membrane (i.e., they exhibit a density peak), but the exact peak location differs. Sodium signal peaks at the phosphate region, while chloride accumulates at the membrane surface.

**KCl.** The density profile of the potassium cation does not exhibit an appreciable peak; nevertheless, potassium does penetrate into the headgroup region. No surface peak is observed for the chloride anion, with penetration into the headgroup region being even weaker.

**NaI.** Sodium cations are enhanced at the phosphate region. Iodide accumulates on the membrane surface and also penetrates deeper into the headgroup region (all the way to the region of negatively charged phosphate groups).

**KI.** Potassium does not exhibit a density peak but penetrates into the headgroup region. Iodide anions are weakly adsorbed on the membrane surface and penetrate deeply the headgroup region (similarly as in the case of NaI).

The ionic density profiles were analyzed in terms of the surface excess, an integral quantity appearing in the Gibbs adsorption isotherm. Evaluated values of the surface excess are as follows:  $\Gamma_{\text{NaCl}} = -0.4$  mol/cm<sup>2</sup>,  $\Gamma_{\text{KCl}} = -1.4$  mol/cm<sup>2</sup>,  $\Gamma_{\text{NaI}} = +0.2$  mol/cm<sup>2</sup>, and  $\Gamma_{\text{KI}} = -0.7$  mol/cm<sup>2</sup>. In agreement with the description of the above-given results, we observed that iodide salts are adsorbed more than chloride salts, from which those with sodium are adsorbed more than those with potassium. Note that the absolute values of Na<sup>+</sup> and K<sup>+</sup> adsorption are somewhat force field dependent; however, the trend that Na<sup>+</sup> is adsorbed more than K<sup>+</sup> is conserved.<sup>11</sup>

Next, we analyzed the changes in the first solvation shell of anions as they approach the headgroup region. The size of the first solvation shell is determined by the location of the first minimum in the radial distribution function (RDF) between the

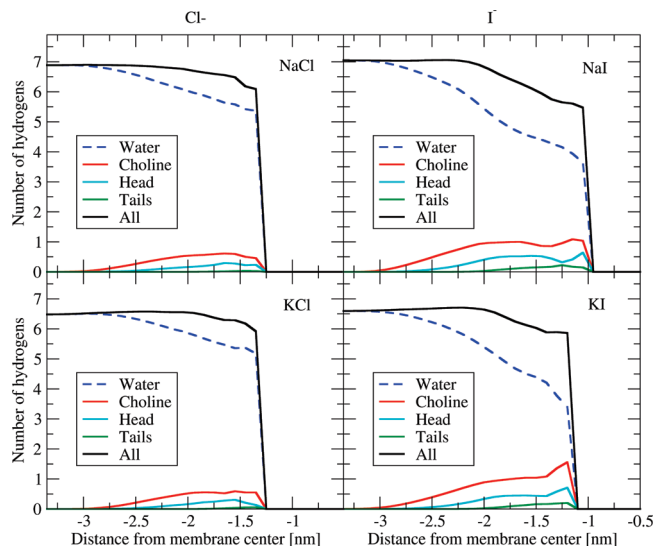


**Figure 2.** Averaged compositions of first solvation shells of chloride and iodide in terms of numbers of water hydrogens, shown along the  $z$ -axis. Partial contributions from water, choline, headgroup except choline, and lipid tails are displayed. Data were averaged over the two equivalent halves of the membrane over 120 ns.

ion and water hydrogens. For chloride the first minimum (following the first maximum) in the RDF is at 0.301 nm, while for iodide it is located at 0.340 nm. The number of hydrogens in the first solvation shell of an anion versus the distance from the membrane center is depicted in Figure 2. The total amount of hydrogens lost from the anionic solvation shell upon entering the membrane is about 1 for iodide but only 0.5 for chloride. The number of water hydrogens that are replaced by lipid atoms is about 2 for iodide and 1 for chloride. Note that iodide at the membrane interface has a significant number of acyl chain hydrogens in its first solvation shell, while chloride does not. Thus, upon entering the headgroup region, iodide is more prepared to shed off water hydrogens from its solvation shell and replace them by lipid atoms. A snapshot showing such a process is presented in Figure 3.

For completeness, we also discuss the situation in the aqueous bulk region of the investigated solutions. There is a small difference in the number of water hydrogens in the first solvation shell of an anion in the aqueous bulk when comparing solutions with different counteranions. This number is about 6.9 for NaCl but 6.5 for KCl and 7.1 for NaI but 6.6 for KI (Figure 2). The decrease due to replacement of sodium by potassium is caused by an increase in ion pairing, as verified via the cation–anion radial distribution functions. The difference between sodium halide and potassium halide radial distribution functions for chloride and iodide is plotted in Figure 4. We see that both anions prefer to pair with potassium over sodium; as a result the integral values shown in the inset of Figure 4 are converging to negative values. The higher tendency of both chloride and iodide to pair with potassium over sodium is in agreement with results of *ab initio* calculations with a polarizable continuum solvent model, as well as with experimental activity coefficients.<sup>16</sup>

To compare the results from our simulations with experiment, we calculated the diffusion constants of lipids, as described previously.<sup>30</sup> The calculated diffusion coefficients for lateral diffusion of lipids are  $(6 \pm 2) \times 10^{-12}$  m<sup>2</sup>/s for NaCl solution,  $(7 \pm 2) \times 10^{-12}$  m<sup>2</sup>/s for NaI solution,  $(6 \pm 2) \times 10^{-12}$  m<sup>2</sup>/s for KCl solution, and  $(11 \pm 4) \times 10^{-12}$  m<sup>2</sup>/s for KI solution. All values lie in the range of experimental values for lipids in

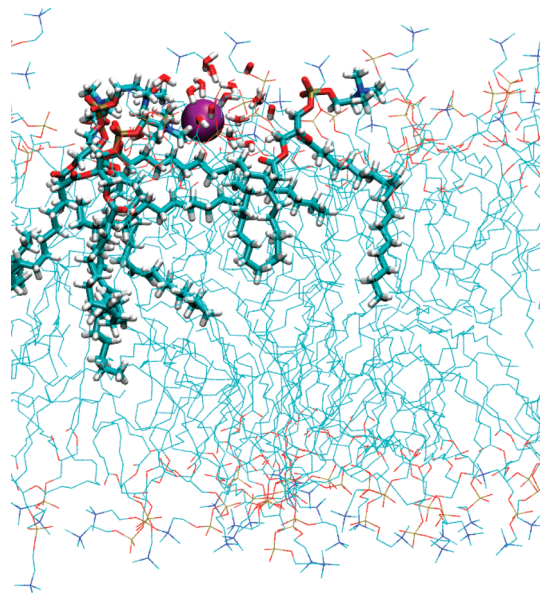


**Figure 3.** A simulation snapshot of iodide adsorbed at a phospholipid membrane surface. The situation illustrates iodide in contact with hydrocarbon chains of lipids surrounded by water and choline groups. Iodide is displayed in purple color and all molecules within 0.6 nm from the iodide are magnified. Remaining water molecules are not shown for clarity and lipids are depicted in lines.

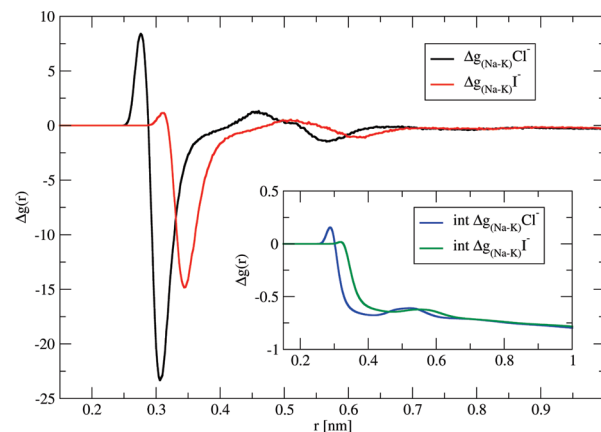


**Figure 4.** Difference in radial distribution functions of sodium vs potassium around chloride (black) and iodide (red) anions. The inset contains the integral values of these differences, showing a preference of potassium over sodium for both anions.

water or salt solution ( $D = (6-7) \times 10^{-12}$  m<sup>2</sup>/s).<sup>11</sup> Unfortunately, the large statistical error in calculations did not allow to perform more direct comparison. Residence times of ions at the membrane interface were evaluated in the same way as in our previous paper.<sup>11</sup> Both anions showed exponential distribution of residence times with a mean value of 50–80 ps. Iodide had longer residence times than chloride in both sodium and potassium salts; however, the differences are within estimated error. Both cations exhibited a power-law distribution of residence times, which were also recently observed in other simulations of membrane in salt solution.<sup>33</sup> The mean residence times for potassium were about 80 ps for both KCl and KI. Sodium mean residence times were roughly 300 and 500 ps in NaCl and NaI solutions.

**Experiment.** The influence of five different monovalent anions ( $\text{Cl}^-$ ,  $\text{Br}^-$ ,  $\text{I}^-$ ,  $\text{ClO}_4^-$ ,  $\text{SCN}^-$ ) on the physical properties of model lipid bilayer was investigated using fluorescence solvent relaxation method. Large unilamellar DOPC vesicles



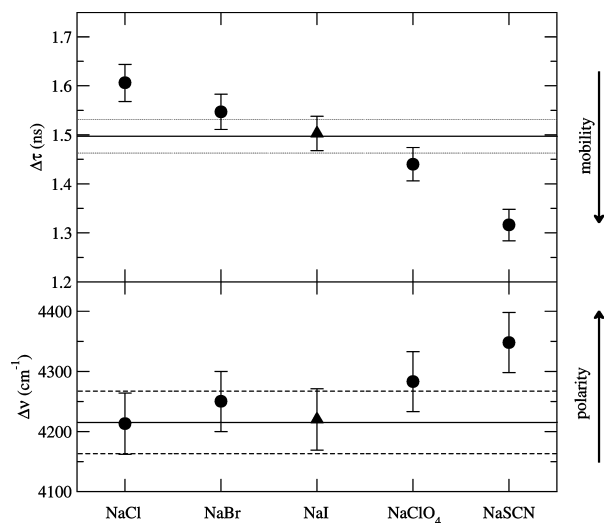


**Figure 5.** Fluorescence solvent relaxation parameters (integrated relaxation time,  $\tau_r$ , and total spectral shift,  $\Delta\nu$ ) obtained for Laurdan embedded in DOPC large unilamellar vesicles suspended in five different salt solutions measured at 10 °C. Salt concentration was 1 M (circles), except for sodium iodide where it was 0.15 M (triangles). Horizontal lines represent values obtained for pure water (dashed lines depict experimental uncertainty).

labeled with Laurdan were suspended in 1 M solution of sodium salts of the above-mentioned anions. Fluorescent polarity probes precisely located in phospholipid bilayer at the level of glycerol have proved to be sensitive to changes in headgroup dynamics and hydration, and hence, indirectly, to lipid packing, protein binding, headgroup tilt, or membrane curvature, to name just a few.<sup>27,28,34</sup>

The results presented in Figure 5 give evidence that, in contrast to small monovalent cations (data not shown), the anions significantly influence relaxation time and total spectral shift measured using Laurdan. The two parameters attributed to mobility and polarity of the lipid bilayer at its glycerol level apparently follow the Hofmeister series<sup>12,35</sup> in the form  $\text{Cl}^- < \text{Br}^- < \text{I}^- < \text{ClO}_4^- < \text{SCN}^-$ . Although the strongest changes are observed in the relaxation time, it is remarkable that the total spectral shift increase of about 150 cm<sup>-1</sup> in the presence of the NaSCN in comparison to water or NaCl solution. It is worth mentioning that the latter effect is rather large when compared to solvent relaxation experiments performed on different systems and topics.

We have shown that already 0.15 M NaCl restricts headgroup mobility, when compared to the bilayer prepared in pure water.<sup>11</sup> Here, for 1 M concentration the effect is only slightly stronger (i.e., relaxation times are 1.56 and 1.61 ns for 0.15 and 1 M NaCl concentrations, respectively), which shows that in the case of sodium chloride, an increased osmolarity does not change bilayer properties dramatically. The polarity in the probe vicinity,  $\Delta\nu$ , does not change upon increasing of NaCl concentration.

From the results shown, it is evident that large soft anions ( $\text{ClO}_4^-$  and  $\text{SCN}^-$ ) increase polarity and mobility at the glycerol level of DOPC bilayer. The increased polarity sensed by Laurdan can be the result of an increased hydration and/or the presence of the ions in the vicinity of the probe. Similar effects are expected for iodide. Unfortunately, at 1 M concentration, quenching of Laurdan fluorescence made solvent relaxation analysis impossible. For this ion, results obtained for 0.15 M concentration are shown. The quenching observed for higher concentrations of iodide confirms iodide penetration down to the glycerol level of phospholipid bilayer.

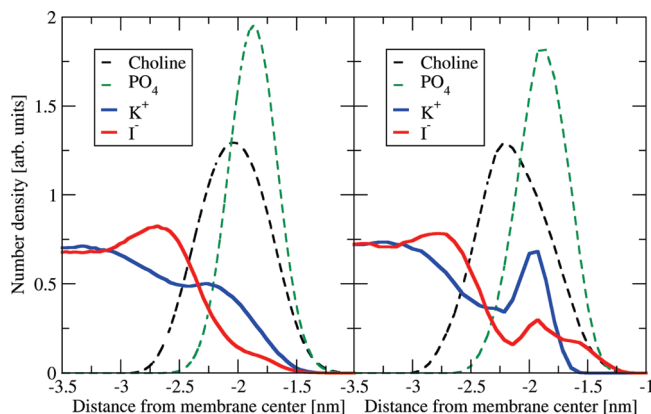


**Figure 6.** Effect of polarizability. Number density profiles for nonpolarizable system are shown on the left side, while the right side depicts the results of polarizable simulation, where larger ion adsorption at the membrane was observed.

## Discussion

In the present simulations, we observed that chloride displays a different behavior compared to iodide at the membrane headgroup region. First of all, we observed that chloride is mostly losing its adsorption peak intensity at the membrane surface, when sodium ion is replaced by the potassium ion as the counterion. There is no such change for the iodide ion; its adsorption peak remains nearly unchanged (see Figure 1). Chloride adsorption at the headgroup region of the lipid bilayer bathed in a NaCl solution is thus caused by the electrostatic attraction to an adsorbed sodium; i.e., it is a counterion effect. In contrast, iodide affinity for the membrane is a genuine effect, independent of the presence of the counterion. The highest intensity of the iodide density peak is observed at the outermost part of the membrane where choline groups are present, which indicates appreciable iodide–choline pairing. This preferable pairing is in agreement with the empirical rule of matching hydration affinities, according to which choline as a weakly hydrated cationic group shall pair with the more weakly hydrated halide anion (i.e., iodide).<sup>14,15</sup>

We also analyzed the differences between chloride and iodide by studying the composition of the anionic first solvation shell. In contrast to density profiles, these results are almost the same for different counterions, Na<sup>+</sup> or K<sup>+</sup>; i.e., the results to a great extent are unbiased by the nature of the counterion. This also reflects the stronger choline pairing with iodide compared to chloride. Moreover, the presence of carbon tails in the first solvation shell of iodide at the membrane demonstrates its affinity for hydrophobic interfaces. This is in agreement with previous studies of iodide at other water/hydrophobic interfaces.<sup>22,24</sup> Since nonpolarizable calculations underestimate anionic propensity for water/hydrophobic interfaces, we also performed a test polarizable simulation, which was computationally very demanding. The comparison between nonpolarizable and test polarizable simulations is shown in Figure 6. As anticipated, polarizability enhances iodide affinity toward the hydrophobic interior of the membrane and, consequently, it also leads to stronger membrane adsorption of potassium (counterion effect). Note that similar polarizable simulation of chloride salt solution will probably lead to increased affinity of chloride toward the membrane; nevertheless, the effect probably will be much smaller than for iodide.

The simulated different behavior at the membrane surface between a relatively small anion, chloride, and larger and softer anion, such as iodide, is supported by the present experimental

results. Fluorescence relaxation spectroscopy shows that soft and large anions (perchlorate and thiocyanate) change mobility and polarity at the glycerol level of DOPC bilayer more than chloride does. Quenching of Laurdan fluorescence by iodide indicates that this anion penetrates into the membrane reaching the vicinity of the probe located at the glycerol level,<sup>36</sup> which is in accord with findings from simulations. On the other hand, this effect is making quantitative solvent relaxation measurements on 1 M iodide impossible. The present results are also in accord with recent experiments on DPPC monolayer with different sodium salts,<sup>9,10</sup> finding that the best-fitting model includes partitioning of sodium cation at the membrane headgroup region with anions adsorption proportional to their size.

On the basis of the above analysis and conclusions from our previous paper<sup>11</sup> that larger cations ( $\text{Cs}^+$ ) adsorb less to the membrane than smaller ones ( $\text{Na}^+$ ), we identify the following determining aspects of ion–lipid membrane interactions:

**1. Ion Pairing.** Salt anions can pair with the positively charged lipid choline group, while cations can create contacts with the negatively charged phosphate group and carbonyl oxygens. In bulk aqueous solutions the tendency for pairing is the highest for ions (charged groups) of opposite charge and matching hydration free energy (i.e., small cations prefer small anions while larger cations pair more with larger anions).<sup>14,15</sup>

**2. Water/Hydrophobic Interface.** The presence of the boundary between water and hydrocarbon chains of lipids implies adsorption of large and polarizable ions. Compared to the affinity of soft anions for the water/vapor interface,<sup>22,24</sup> this effect is reduced at the lipid membrane surface due to the presence of negatively charged groups of the lipid headgroups.

**3. Steric Hindrance.** The amount of water is rapidly decreasing upon moving from the solution to the headgroup region; moreover, water at the interface is strongly interacting with the lipid headgroups. This has consequences especially for the mobility and other dynamical properties.

**4. Counterion Attraction.** Salt ions of opposite charge tend to screen each other, and therefore, adsorption of one type of them at the membrane interface leads to the attraction of counterions.

The above reasoning leads to the following prediction: small cations ( $\text{Na}^+$ ) should be attracted to the membrane, while larger cations ( $\text{Cs}^+$ ) should not. However, even larger “hydrophobic” cations (such as tetraalkylammonium cations) are expected to be adsorbed at a membrane surface, but for a different reason: the ion hydrophobicity. Larger anions (e.g., iodide, perchlorate, and thiocyanate) adsorb to the membrane more than smaller ones (chloride) due to their size, polarizability, and ion pairing with choline group of the membrane.

## Conclusions

We have investigated the properties of different salt solutions at the interface of DOPC membrane by means of molecular dynamics simulations and fluorescence spectroscopy. We have observed a difference in the adsorption properties of anions ( $\text{Cl}^-$  vs  $\text{I}^-$ ) which follows the Hofmeister series.<sup>12,35</sup> The existence of such a difference has been suggested based on the results from the previous experiments on vesicle swelling,<sup>7</sup> but the difference was less significant in the previous studies of membranes with sodium salts.<sup>9–11</sup> The use of potassium salts in the present study strongly underlines the differences between anions. By evaluating the composition of the first solvation shell of anions, as they adsorb at the membrane surface, we were able to identify clearly the difference between chloride and iodide, the latter being less influenced by a particular counter-

cation. In addition, in our pioneering polarizable calculations we showed that the effect of polarizability leads to a stronger adsorption of iodide to the hydrophobic membrane interface. The above results are in agreement with solvent relaxation experiments.

The present study allowed us to identify mechanisms of ion–membrane interaction (i.e., ion pairing within the membrane, presence of the water/hydrophobic interface, and counterion effects). Our results are in accord with the previous measurements performed in phospholipids membranes, as well as with the measurements performed in experiments on ion pairing in salt solutions,<sup>1–3,5,8,11</sup> which led to an establishment of the rule of preferable ion pairing for ions with matching water affinities.<sup>14,15</sup> We suggest that the above-mentioned mechanisms are more general and, therefore, are also at work for other biomolecular systems containing salt solutions, thus shedding more light on the molecular foundations of ion specificity, as expressed by the Hofmeister series.<sup>12,35</sup>

**Acknowledgment.** We thank Valery Andrushchenko and Petr Bouř for valuable discussions. Support from the Czech Ministry of Education (grant LC512) and the Czech Science Foundation (grant 203/08/0114) is gratefully acknowledged. R.V. acknowledges support from the International Max-Planck Research School. Part of the work in Prague was supported via Project Z40550506. M.L.B. acknowledges the support of the Office of Naval Research.

## References and Notes

- (1) Pandit, S. A.; Bostick, D.; Berkowitz, M. L. *Biophys. J.* **2003**, *84*, 3743–3750.
- (2) Bockmann, R. A.; Hac, A.; Heimbürg, T.; Grubmüller, H. *Biophys. J.* **2003**, *85*, 1647–1655.
- (3) Sachs, J. N.; Nanda, H.; Petrache, H. I.; Woolf, T. B. *Biophys. J.* **2004**, *86*, 3772–3782.
- (4) Sachs, J. N.; Woolf, T. B. *J. Am. Chem. Soc.* **2003**, *125*, 8742–8743.
- (5) Gurtovenko, A. A.; Vattulainen, I. *J. Phys. Chem. B* **2008**, *112*, 1953–1962.
- (6) Garcia-Celma, J. J.; Hatahet, L.; Kunz, W.; Fendler, K. *Langmuir* **2007**, *23*, 10074–10080.
- (7) Petrache, H. I.; Zemb, T.; Belloni, L.; Parsegian, V. A. *Proc. Natl. Acad. Sci. U.S.A.* **2006**, *103*, 7982–7987.
- (8) Leontidis, E.; Aroti, A.; Belloni, L.; Dubois, M.; Zemb, T. *Biophys. J.* **2007**, *93*, 1591–1607.
- (9) Leontidis, E.; Aroti, A. *J. Phys. Chem. B* **2009**, *113*, 1460–1467.
- (10) Leontidis, E.; Aroti, A.; Belloni, L. *J. Phys. Chem. B* **2009**, *113*, 1447–1459.
- (11) Vácha, R.; Siu, S. W. I.; Petrov, M.; Bockmann, R. A.; Jurkiewicz, P.; Barucha-Kraszewska, J.; Hof, F.; Berkowitz, M. L.; Jungwirth, P. *J. Phys. Chem. B* **2009**, *113*, 7235–7243.
- (12) Kunz, W.; Henle, J.; Ninham, B. W. *Curr. Opin. Colloid Interface Sci.* **2004**, *9*, 19–37.
- (13) Berkowitz, M. L.; Bostick, D. L.; Pandit, S. *Chem. Rev.* **2006**, *106*, 1527–1539.
- (14) Collins, K. D. *Biophys. J.* **1997**, *72*, 65–76.
- (15) Collins, K. D. *Biophys. Chem.* **2005**, *119*, 10.
- (16) Jagoda-Cwiklik, B.; Vácha, R.; Lund, M.; Srebro, M.; Jungwirth, P. *J. Phys. Chem. B* **2007**, *111*, 14077–14079.
- (17) Vlatchy, N.; Jagoda-Cwiklik, B.; Vácha, R.; Touraud, D.; Jungwirth, P.; Kunz, W. *Adv. Colloid Interface Sci.* **2009**, *146*, 42–47.
- (18) Kalcher, I.; Horinek, D.; Netz, R. R.; Dzubiella, J. *J. Phys.: Condens. Matter* **2009**, *21*, 424108–424118.
- (19) Hess, B.; van der Vegt, N. F. A. *Proc. Natl. Acad. Sci. U.S.A.* **2009**, *106*, 13296–13300.
- (20) Fennell, C. J.; Bizjak, A.; Vlatchy, V.; Dill, K. A. *J. Phys. Chem. B* **2009**, *113*, 6782–6791.
- (21) Lund, M.; Jagoda-Cwiklik, B.; Woodward, C. E.; Vácha, R.; Jungwirth, P. *J. Phys. Chem. Lett.* **2009**, *1*, 300–303.
- (22) Vrbka, L.; Mucha, M.; Minofar, B.; Jungwirth, P.; Brown, E. C.; Tobias, D. J. *Curr. Opin. Colloid Interface Sci.* **2004**, *9*, 67–73.
- (23) Jungwirth, P.; Tobias, D. J. *J. Phys. Chem. B* **2002**, *106*, 6361–6373.
- (24) Jungwirth, P.; Tobias, D. J. *Chem. Rev.* **2006**, *106*, 1259–1281.

- (25) Dang, L. X. *J. Phys. Chem. B* **2002**, *106*, 10388–10394.
- (26) Dang, L. X.; Chang, T. M. *J. Phys. Chem. B* **2002**, *106*, 235–238.
- (27) Sykora, J.; Jurkiewicz, P.; Epand, R. M.; Kraayenhof, R.; Langner, M.; Hof, M. *Chem. Phys. Lipids* **2005**, *135*, 213–221.
- (28) Jurkiewicz, P.; Olzynska, A.; Langner, M.; Hof, M. *Langmuir* **2006**, *22*, 8741–8749.
- (29) Van Der Spoel, D.; Lindahl, E.; Hess, B.; Groenhof, G.; Mark, A. E.; Berendsen, H. J. *J. Comput. Chem.* **2005**, *26*, 1701–1718.
- (30) Siu, S. W. I.; Vacha, R.; Jungwirth, P.; Bockmann, R. *J. Chem. Phys.* **2008**, *128*, 125103.
- (31) Caldwell, J. W.; Kollman, P. A. *J. Phys. Chem.* **1995**, *99*, 6208–6219.
- (32) Dang, L. X.; Schenter, G. K.; Glezakou, V. A.; Fulton, J. L. *J. Phys. Chem. B* **2006**, *110*, 23654.
- (33) Miettinen, M. S.; Gurtovenko, A. A.; Vattulainen, I.; Karttunen, M. *J. Phys. Chem. B* **2009**, *113*, 9226–9234.
- (34) Sheynis, T.; Sykora, J.; Benda, A.; Kolusheva, S.; Hof, M.; Jelinek, R. *Eur. J. Biochem.* **2003**, *270*, 4478–4487.
- (35) Hofmeister, F. *Arch. Exp. Pathol. Pharmacol.* **1888**, *24*, 247–260.
- (36) Barucha-Kraszewska, J.; Kraszewski, S.; Jurkiewicz, P.; Ramseyer, C.; Hof, M. *Biochim. Biophys. Acta* **2010**. doi: 10.1016/j.bbamem.2010.05.020. JP102389K